ELSEVIER

Wear 186–187 (1995) 368–374

WEAR

Water droplet erosion and microstructure of laser-nitrided Ti–6Al–4V

C. Gerdes [a], A. Karimi [b], H.W. Bieler [c]

[a] *ABB—Kraftwerke AG, KWRM.T, CH-5401 Baden, Switzerland*

[b] *Institut de Génie Atomique, Ecole Polytechnique Fédérale de Lausanne, CH-1015 Lausanne, Switzerland*

[c] *Sulzer Innotec AG, Werkstoffe und Oberflachen, CH-8404 Winterthur, Switzerland*

Abstract

The ability of laser nitriding to improve water droplet erosion resistance of Ti–6Al–4V alloy was studied. Using a CO_2 continuous laser, a layer of about 400 μm thickness was nitrided and another layer of 400–500 μm was only heat affected. Electron microscopy observations showed that the microstructure of nitrided layers consists essentially of TiN compounds which are embedded in Ti(α) matrix. Depending on the nitrogen concentrations within the feeding gas, the titanium nitrides exhibited plate-like shape or dendritic morphologies. Below the nitrided layer a thickness of 50–100 μm of samples underwent martensitic structure which in its turn gives rise progressively to bimodal (α+β) base material. Laser nitriding increased microhardness from 370–400 to 650–800 kgf mm^{-2}, and enhanced erosion resistance significantly compared with untreated Ti–6Al–4V and hardened 12% Cr stainless steel. The mechanism of material removal by erosion was changed from work hardening and platelets detachment in untreated samples to brittle fracture by formation of large flakes and spalling in nitrided layers. Advanced stages of erosion are accompanied by the appearance of macrocracks often in the nitrided zone, but some of them propagate even into heat-affected area. The annealing at 650 and 700 °C of the laser-nitrided samples results in precipitation of β phase rich in vanadium.

Keywords: Erosion; Water droplets; Ti–6Al–V; Lasers; Nitriding

1. Introduction

The excellent high strength-to-weight ratio and corrosion resistance of the titanium alloy Ti–6Al–4V has for many years highlighted it as an attractive material for aircraft and steam turbine design (L-1 row), but most important would be the advantage for the last stage blade (L-0) of a steam turbine substituting chromium stainless steels. In such an application the materials are exposed to severe erosive wear due to water droplet impingement. The studies on rain erosion and water droplet damages revealed that under a wide range of test conditions, titanium alloy Ti–6Al–4V exhibits roughly comparable erosion resistance to 12% Cr steels [1–3]. In contrast to the 12% Cr steel the Ti alloys cannot be hardened to a great extent by quenching in order to improve the water droplet erosion resistance sufficiently [4].

To strengthen titanium alloys, nitriding has been found to be one of the most promising methods which provides an efficient increase of hardness to the surface owing to formation of TiN dendrites [5,6]. Recently, laser processing techniques have been widely used instead of conventional nitriding methods such as gaseous nitrogen, salt bath or ion nitriding, which require higher global temperatures and extensive hours of processing. The laser nitriding process leads commonly to formation of titanium nitrides TiN_x within the matrix Ti(α)-N solid solution [7,8]. Such a modification of composition and microstructure results in a higher degree of hardening and thicker nitrided layers compared with other techniques mentioned above.

Several studies have dealt with the tribological behaviour of laser-nitrided Ti–6Al–4V alloy. Yerramareddy et al. [4] conducted erosive and sliding wear tests on as-received, laser-melted and laser-nitrided specimens. They observed that only laser nitriding reduced erosion rate several times under impingement of fine erosive solid particles. However the laser treatments did not have any effect on the erosion resistance, in particular, when the specimens were impacted by coarse particles at higher velocities. In contrast, Molian et al. [9] measured a substantial reduction of sliding wear rate by up to two orders of magnitude in laser-cladded and heat treated samples. Sue et al. [10] showed that residual stress plays a major role on erosion resistance of such layers.

The objective of this work is to study water droplet erosion behaviour of laser-nitrided Ti–6Al–4V samples. The microstructural changes and surface modifications as well as the erosion mechanisms will be observed using scanning and transmission electron microscopy. The results will be discussed with respect to erosion test behaviours.

SSDI 0043-1648(95)07153-9

2. Experimental details

The material tested was a Ti–6Al–4V alloy with a bimodal ($\alpha+\beta$) microstructure. Laser gas nitriding was carried out using a continuous wave CO_2 gas laser 1.5 kW with a circular beam and Gaussian energy distribution. Nitrogen gas was introduced into the melt pool through inert gas (Argon) shrouding. An appropriate flow rate and stream size of feeding gas (N_2+Ar) can avoid oxygen contamination of the substrates. The nitrogen pick-up was dependent on the partial pressure of N_2 in the (N_2+Ar) gas stream. In this work the ratio of the partial pressure between N_2 and Ar was varied within the range of N_2:Ar = 1:4 to 1:2. A series of beam passes of 1.3 mm width with around 50% overlap were made providing a melted depth of approximately 0.5 mm.

The water droplet erosion tests were performed in an erosion test-rig which is basically a rotating arm [11]. The rectangular eroding specimens are mounted at its tips. The arm is installed in a chamber which can be evacuated to about 0.1 atm to avoid heating of the specimens due to air friction and to obtain high velocities. A liquid drop generator is fixed at the circumference of the chamber to provide three water streams parallel to the specimen surface in order to produce 90° impact cycles. The intensity of impacts can be adjusted by rotation velocity of the rotor. For the results discussed in this paper, droplet size was kept fixed at 0.2 mm but velocity of impingement was varied between 300 and 500 m s^{-1}.

3. Experimental results

3.1. Surface modifications

Basic observations on metallurgical aspects of the laser process such as solidification texture and induced microstructure showed that the nitrided samples exhibit commonly three distinct regions. An example of such modifications is illustrated in Fig. 1 which corresponds to transverse cross-section of a nitrided sample. The melted and re-solidified zone with a thickness of about 400 μm consists essentially of TiN_x compounds embedded in Ti(α) matrix (Fig. 1, region A). The X-ray diffraction spectrometry confirmed that a notable quantity of Ti(β) is present in this region. Morphology and distribution of the nitrides depend on the process parameters and nitrogen concentration in the feeding gas. In general, nitrogen is dissolved very rapidly in the molten titanium and rapid mixing is ensured by the vigorous convection. Thus, the melted layers show roughly an uniform distribution of nitrides. Below the nitrided zone, a layer of 50–100 μm undergoes martensitic transformation with long needles grown from β phase similar so that produced by conventional quenching. These martensites give rise progressively to ($\alpha+\beta$) phases of the base metal. Owing to temperature gradient in this layer, their microstructural feature varies according to time–temperature history of different areas. Transition from martensite to bimodal ($\alpha+\beta$) occurs through a layer of 300–350 μm as illustrated by region B in Fig. 1. The region C corresponds to unaffected base material.

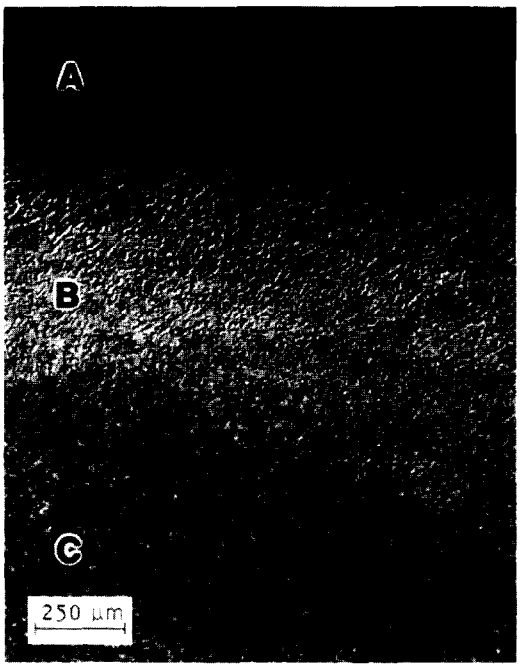

Fig. 1. Transverse cross-section of a laser-nitrided Ti–6Al–4V sample: A is laser-nitrided zone. B is laser heat affected zone relating transition from martensite to ($\alpha+\beta$) base material. C relates bimodal ($\alpha+\beta$) base material.

3.2. Erosion tests

The results of erosion tests performed on the as-received Ti–6Al–4V specimens for different conditions are presented in Fig. 2(a) which depicts the volume loss as a function of the number of impingements. In order to provide a realistic comparison on the behaviour of Ti–6Al–4V, the data measured on 12% Cr stainless steel are also reported on the diagram. For droplet size of 0.2 mm, the 12% Cr steel exhibits a slightly higher erosion strength and a notably longer incubation time at higher impingement velocities (400–500 m s^{-1}). In contrast, the titanium alloy shows a better behaviour at the lowest velocity (300 m s^{-1}). This behaviour of alloys under droplet impact is similar to that observed under fatigue tests, even the sample stressing under erosion is different from that under fatigue. In fact, the 12% Cr steel appeared more strength to cyclic fatigue with higher stress amplitude compared with Ti–6Al–4V which lead to longer fatigue life time at lower amplitudes. The repeated droplet impingements induce localized repeated plastic deformation in the surface which can be assumed to be similar to cyclic deformation under fatigue test.

The effect of hardening on erosion behaviour of both alloys is illustrated in Fig. 2(b) for a velocity of 400 m s^{-1}. The Cr steel was hardened by quenching, and titanium alloy was laser nitrided. The cumulative volume loss vs. number of impacts shows that laser nitriding increased incubation time of tita-

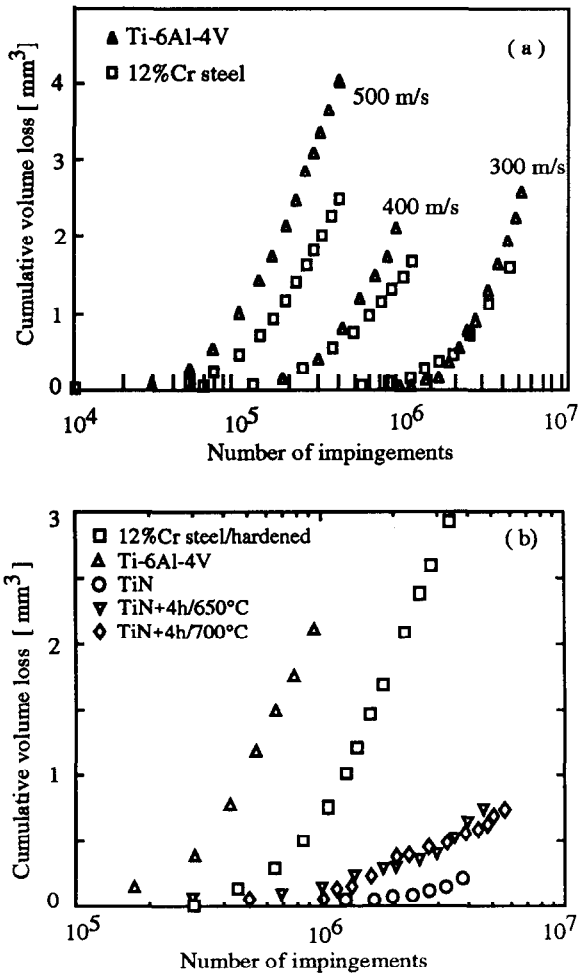

Fig. 2. Cumulative volume loss versus number of droplet impingements: (a) comparison of untreated Ti–6Al–4V with 12% Cr stainless steel (b) effect of laser nitriding and additional annealing on erosion rate at velocity of 400 m s^{-1}.

nium alloy about one order of magnitude and also decreased notably its erosion rate. The improvement brought about by hardening of stainless steel seems to be much lower compared with that produced by laser nitriding. The incubation time in steel was increased only 2–3 times compared with untreated steel and the volume loss was recorded sensitively higher than nitrided Ti–6Al–4V.

As regards with titanium alloy, some of the nitrided specimens were subjected to additional annealing 4 h at 650 °C or 700 °C. According to Fig. 2(b) such heat treatment reduced only slightly incubation time as compared with unannealed samples. The erosion rate remained almost the same.

3.3. Erosion mechanism

The examples of the feature of damage corresponding to an advanced stage of erosion are shown in Fig. 3 for both untreated and laser-nitrided samples. The micrographs (a) and (b) show scanning electron microscopy observations of the eroded surface, while micrographs (c) and (d) depict transverse cross-sections of the same specimens. Erosion occurs by formation of deep craters characterized by a mean diameter of about 0.3–0.4 mm and spacing interval of 0.5–0.8 mm in untreated sample. Depth of the craters reach 500 μm. Contrary to untreated alloy, the laser-nitrided specimens did not undergo crater formation. The typical feature of droplet erosion in this case arises by the appearance of long macro-cracks parallel to the droplet stream (Fig. 3(b)). These cracks were initiated, in general, within the nitrided layers during incubation period and propagated inside the specimen during advanced erosion periods. A substantial part of the material loss occurs, in general, from these cracks.

In order to detect damage propagation in the subsurface layers, the transverse cross-section of the eroded specimens was observed (Figs. 3(c) and 3(d)). The related results suggest that the material loss in untreated specimens occurs subsequent to progressive work hardening without formation of any macro-crack around the craters (Fig. 3(c)). At the same time, laser-treated samples exhibit macro-cracks often within the laser-melted area as indicated by arrows in Fig. 3(d). Some of the cracks are extended to laser-heated regions and can reach even non-heat-affected base material. The formation of these cracks can be related to the low ductility of the nitrided layer and the presence of high residual stresses within the laser-affected layer owing to added alloying and shrinkage of the melt during solidification. However, these cracks seem not to have a great influence on the erosion behaviour of the nitrided samples, probably because of localized character of stressing. They should affect the bulk mechanical properties such as fatigue strength. For this reason heat treatments were conducted on the nitrided samples as described in Section 3.4 to observe whether or not crack initiation and propagation may be influenced.

Differences in the microstructures and properties of untreated and nitrided samples lead to two distinct material removal mechanisms. The untreated samples being more ductile undergo some amount of plastic deformation under impingement of water droplets. Consequently damage at early stages of erosion consists of shallow craters on the surface due to plastic deformation. The accumulation of impacts with exposure time results in overlapping of impact craters and delamination of plastically deformed layers. The progressive work hardening increases the probability of local fractures and leads to the detachment of thin platelets. On the contrary, high hardness, low ductility and greater internal stress of laser-treated samples increase crack sensitivity of the nitrided layers by reducing their capacity to plastic deformation. Under high intensity impacts material removes by brittle fracture leading to formation of large flakes (Fig. 4(a)). The accumulation of impingements results in the propagation of multiple subsurface cracks which can cause loss of bigger fragments when they cross together (Fig. 4(b)). In spite of these effects of cracking, the erosion resistance of the nitrided layers is much higher than for untreated samples (Fig. 2). This allows to suggest that the strengthening provided by laser nitriding against droplet impact

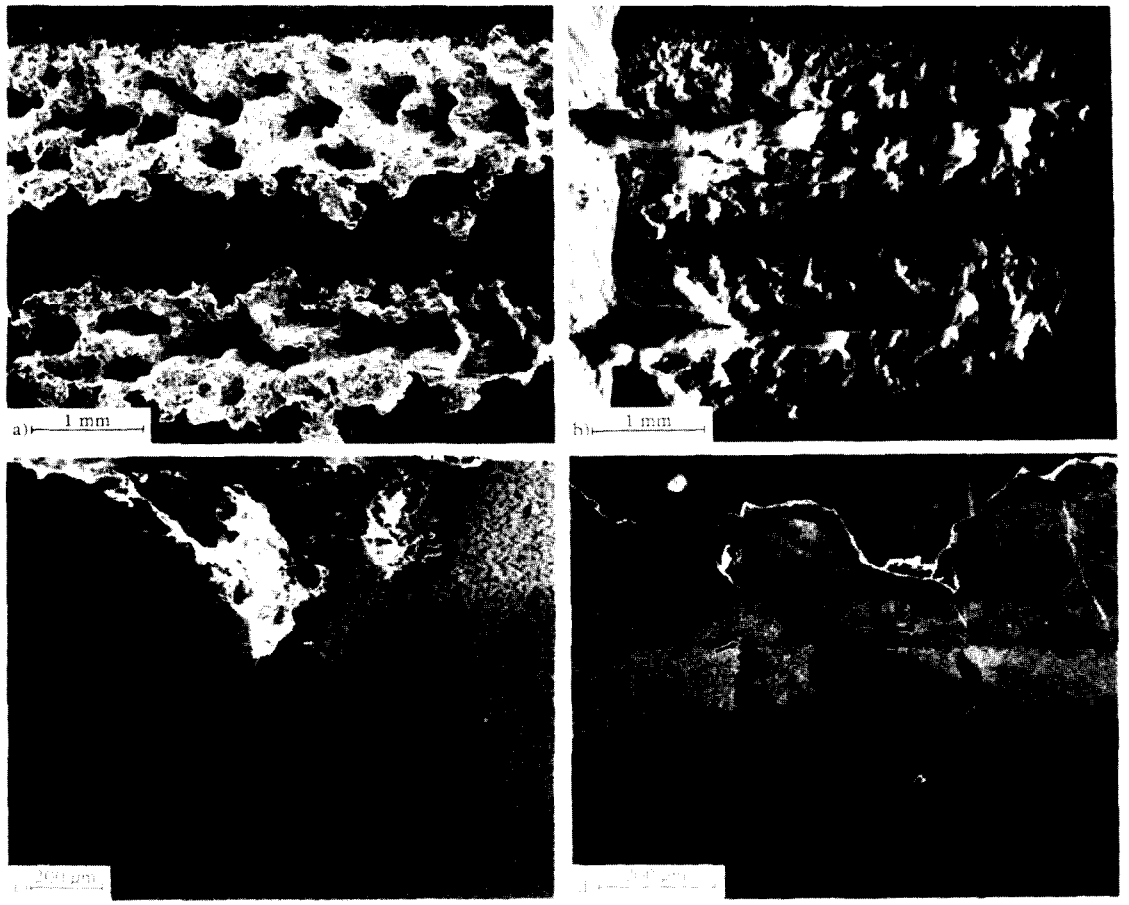

Fig. 3. Comparison of material removal in as-received and laser-nitrided Ti–6Al–4V: (a) ductile erosion and formation of craters in untreated sample; (b) brittle erosion in nitrided sample; (c) cross-section of untreated sample; (d) cross-section of a nitrided specimen showing cracks induced by water droplet impacts (see arrows).

stressing increases the incubation time to a great extent. The deleterious effect of the cracking does not play the major role for erosion damage of the nitrided layers.

3.4. Heat treatment

To reduce crack sensitivity of the laser-nitrided samples under an external applied stress, heat treatments at 650 °C and 700 °C were conducted. In spite of the relatively low temperatures used, a significant microstructural change occurred in both of the laser-nitrided and heat-affected regions. For a better understanding of such heat treatment effect, several micrographs corresponding to morphological details of laser-nitrided sample followed by an annealing are shown in Fig. 5. The typical microstructure of a laser-nitrided layer consists of titanium nitride (TiN_x) precipitates embedded in Ti(α) matrix. Nitrogen is a strong alpha stabilizer and can be extensively solved in the alpha phase over a

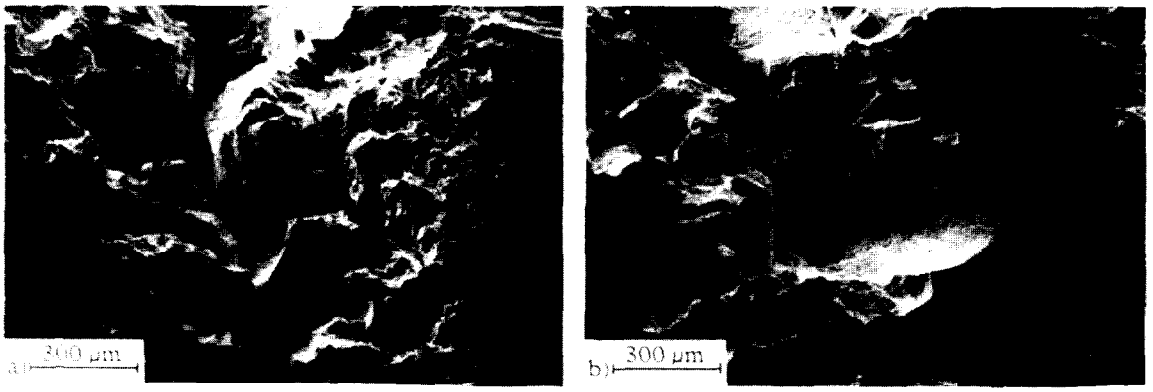

Fig. 4. Mechanism of erosion in nitrided layer: (a) occurrence of macro-cracks and large flakes; (b) spalling and brittle character of material loss.

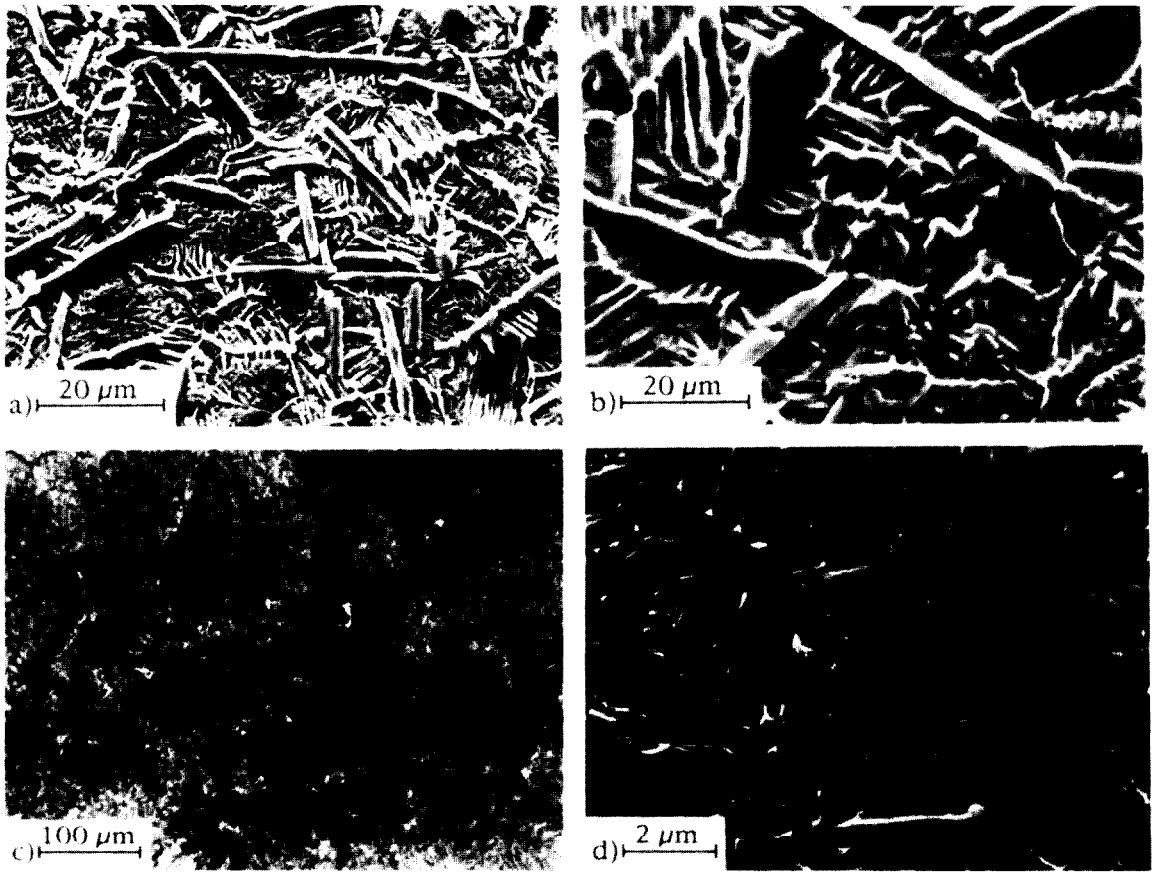

Fig. 5. Effect of heat treatment on laser-nitrided layer: (a) microstructure before heat treatment; (b) Ti(α) needles and TiN interfaces become diffused after heat treatments; (c) recrystallization in nitrided layer; (d) vanadium rich precipitates, β phase.

wide range of concentration. For this reason, after complete re-solidification of samples, both primary alpha and beta titanium were transformed to fine alpha needles (Fig. 5(a)). The titanium nitride TiN has also a wide range of nitrogen solubility from ≈28 to 50 at.% according to Ti–N phase diagram. The content of nitrogen in the feeding gas and the parameters of laser processing control different morphology of titanium nitride. The higher contents of nitrogen lead to formation of dendrites [12], and lower contents give rise to appearance of plate-like shapes which are visible on micrograph 5(a).

The main modifications induced after 4 h of annealing at 650 and 700 °C are summarized in Figs. 5(b)–5(d). One of the microstructural effects is homogenizing tendency between alpha stabilizer phases owing to diffusion of solid solution elements. The nitrides and Ti(α) needles revealed by a chemical etching are more diffused in annealed samples than untreated specimens which show sharp interfaces (Figs. 5(a) and 5(b)). Another effect is the recrystallization which occurs within both laser-nitrided and heat-affected layers by formation of grains with 20–100 μm diameter (Fig. 5(c)). However, the most prominent feature of modification is the appearance of uniformly distributed precipitates which are very rich in vanadium (Fig. 5(d)). The lower solubility of vanadium in Ti(α) may be the cause of such transformation [13].

3.5. Microhardness

The effect of post heat treatments on hardness of laser-nitrided samples was studied, using a Vickers microindenter coupled with a computer which records loading–unloading penetration curve. The examples of the hardness profile obtained for a nitrided specimen and additionally annealed specimen 4 h at 650 °C or 700 °C are reported in Fig. 6. The microhardness values were found rather scattered, in particular, for unannealed samples. To give an efficient comparison here, only the mean values of data are recorded. Each curve corresponds to about 60–70 indentations.

The bimodal (α+β) base material showed originally a hardness varying between 370–400 kgf mm^{-2}. After laser treatment, the nitrided layer obtained a hardness laying in most of the cases at the range of 700–800 kgf mm^{-2} (Fig. 6). These higher values of hardness decrease rapidly over a narrow band of thickness of about 100–150 μm which corresponds to martensitic zone laying just below nitrided layer. Beyond this area in the laser heat-affected zone, the hardness remains practically stable and shows the same values as the initially (α+β) alloy. In addition to above details, it should

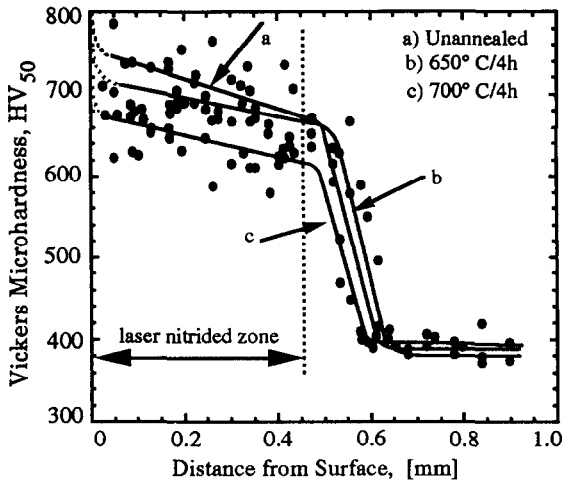

Fig. 6. Microhardness profile of a laser-nitrided samples along the transverse cross-section: (a) without heat treatment; (b) annealing 4 h at 650 °C; (c) annealing 4 h at 700 °C.

be noted that the laser-nitrided surface shows a thin layer of 2–3 μm TiN on the surface which has higher microhardness reaching 1300–1350 kgf mm^{-2}. This surface microhardness is shown in diagram Fig. 6 by the discontinuous lines.

Annealing of the specimens during 4 h at 650 or 700 °C modified slightly hardness of the nitrided layers. The range of microhardness measured for 650 and 700 °C annealings were respectively 630–760 and 600–680 kgf mm^{-2}. Such a softening of the nitrided layer can be related to some amount of recovery within the Ti(α) needles and to diffusion of solid solution elements, in particular, nitrogen and vanadium to form dense precipitates as shown in Fig. 5(d). The laser heat-affected layer and (α + β) base metal did not undergo any detectable hardness modification after heat treatment.

4. Discussion

The industrial trend towards steam turbines of greater output and higher efficiency favours use of titanium alloys to increase length of the last stage blades. This in its turn increases erosion risk of the components owing to higher velocity impingement of water droplets. At higher velocities of impingement the titanium alloy Ti–6Al–4V shows a relatively poor erosion resistance compared with the hardened 12% Cr stainless steel (Figs. 2(a) and 2(b)). To overcome severe erosion damage, titanium alloys have been subjected to structural modification strengthening.

One of the most promising methods to improve wear behaviour of titanium alloys is the laser surface alloying with nitrogen, carbon or boron [8,14,15]. Among these alloying elements, the laser nitriding has attracted more attention because of best balance between increased hardness and decreased ductility and several works have dealt with the feasibility of the method and related properties [7,12,16]. The data available in the published works on laser nitriding characteristics and mechanical behaviour modification of Ti–6Al–4V, provide a confused and sometime contradictory conclusions. These may be related to the effects of processing variables on the nature and morphology of the hardened layer, or to different stressing parameters under experimental test conditions.

Nevertheless, the sliding and scuffing wear resistance was found to be improved owing to increased hardness and the formation of wear resistant compounds [4,12]. In contrast, fatigue limit was decreased owing to elevated residual stress and crack sensitivity [14]. The solid particle erosion did not show any appreciable effects following to laser nitriding, in particular, at higher velocities [4,17]. In addition, the mechanism of material removal remained the same for untreated and nitrided alloys involving ploughing, flake formation and lip fragmentation. The marked improvements brought about by laser nitriding were observed on abrasive wear tests [9,15]. The formation of TiN compounds and high hardness of nitrided layer were considered to be responsible of such an effect. As the material loss occurs essentially by ploughing, the increased surface hardness rises the resistance to penetration and thereby the strength to abrasion.

Material stressing under impingement of water droplets is significantly different from the other wear situations mentioned above. The hardness alone is not a major parameter to correlate droplet erosion resistance contrary to abrasion or sliding wear. Toughness, work hardenability and fatigue strength are the important properties which influence a great deal liquid impact erosion [18,19]. On the basis of such criteria, the laser nitriding performed in this work was chosen to produce a medium hardness (650–800 kgf mm^{-2}) to avoid formation of brittle structures and to lower the crack growth sensitivity. It has been shown experimentally that higher hardnesses in laser-nitrided layer is synonymous with crack propagation during solidification [7,16]. At present work the risk of crack initiation was considerably reduced by annealing of the samples 4 h at 650 or 700 °C. However the erosion behaviour and microhardness values remained similar.

5. Conclusions

Laser nitriding of Ti–6Al–4V modifies bimodal (α + β) structure of base material into a composite made coarsely of TiN compound embedded in Ti(α) matrix.

Water droplet erosion behaviour was improved, in particular by increasing duration of incubation period.

Material removal mechanisms were changed from work hardening and platelets detachment in untreated samples, to brittle fracture and large flake formation in laser-nitrided layers.

Annealing of nitrided samples at 650 and 700 °C decreased residual stress and resulted in recrystallization and formation of vanadium rich precipitates of β phase.

Owing to annealing the surface hardness and the erosion resistance were only slightly reduced.

Acknowledgements

The authors wish to thank Ch. Triscornia for assistance in electron microscopy observations. The Swiss Priority Program on Materials (PPM) is acknowledged for financial support of the project.

References

[1] R. Araki, M. Kisimoto and K. Yoshida, Evaluation of titanium blade erosion in low-pressure steam turbine, *JSME Int. J. Series II, 34* (3) (1991) 397–403.

[2] H.W. Meyer, H. Bratsch and U. Wieland, Long-term experience and development with titanium blades for advanced steam turbines, in R.I. Jaffee (ed.), *Proc. Workshop on Titanium Steam Turbine Blading, 9–10 November 1988, Palo Alto, CA, EPRI ER-6538*, Pergamon, New York, 1990, pp. 30–43.

[3] N. Yasugahira, K. Namura, R. Kaneko and T. Satoh, Erosion resistance of titanium alloys for steam turbine blades as measured by water droplet impingement, in R.I. Jaffee (ed.), *Proc. Workshop on Titanium Steam Turbine Blading, 9–10 November 1988, Palo Alto, CA, EPRI ER-6538*, Pergamon, New York, 1990, pp. 385–401.

[4] S. Yerramareddy and S. Bahadur, The effect of laser surface treatments on the tribological behaviour of Ti–6Al–4V, *Wear, 157* (1992) 245–262.

[5] W. Lengauer, The titanium–nitrogen system: A study of phase reactions in the subnitride region by means of diffusion couples, *Acta Metall. Mater., 39* (12) (1991) 2985–2996.

[6] X. Qiu, J.R. Conrad, R.A. Dodd and F.J. Worzla, Plasma source nitrogen ion implantation of Ti–6Al–4V, *Metall. Trans. A, 21A* (1990) 1663–1667.

[7] O.V. Akgun and O.T. Inal, Laser surface melting of Ti–6Al–4V alloy, *J. Mater. Sci., 27* (1992) 1404–1408.

[8] A. Walker, J. Folkes, W.M. Steen and D. West, Laser surface alloying of titanium substrates with carbon and nitrogen. *Surf. Eng., 1* (1) (1985) 23–29.

[9] P.A. Molian and L. Hualun, Laser cladding of Ti–6Al–4V with BN for improved wear performance, *Wear, 130* (1989) 337–352.

[10] J.A. Sue and H.H. Troue, Influence of residual compressive stress on erosion behaviour of arc evaporation titanium nitride coating, *Surf. Coat. Technol., 36* (1988) 695–705.

[11] C.M. Maggi, *Werkstoffprüfung, DVM, 3–4* (1987) 197–204.

[12] P.H. Morton, T. Bell and B.L. Mordike, Laser gas nitriding of titanium and titanium alloys, in T.S. Sudarshan and J.F. Braza (eds.), *Proc. 5th Int. Conf. on Surface Modification Technologies, Birmingham, UK, 2–4 September 1991*, The Institute of Materials, Vol. V, 1992, pp. 593–609.

[13] M.K. McQuillan, Phase transformations in titanium and its alloys, *Met. Rev., 8* (29) (1963) 41–104.

[14] B.L. Mordike, Laser gas alloying, in C.W. Drapper and P. Mazzoldi (eds.), *Proc. NATO Advanced Study Institute on Laser Treatment of Metals, San Miniato, Italy, September 2–13, 1985*, Martinus Nijhoff, Dordrecht, 1986, pp. 389–412.

[15] M. Collin, J.P. Massoud and G. Coquerelle, Elaboration de ceramiques par laser continu sur l'alliage TA6V, *Ann. Chim. Sci. Mater., 13* (4–5) (1988) 327–335.

[16] L. Jianglong, L. Qiquan and Z. Zhirong, Laser gas alloying of titanium alloy with nitrogen, *Surf. Coat. Technol., 57* (1993) 191–195.

[17] T. Duverneix, T. Puig and F. Bataille, Laser nitriding of titanium by solid state diffusion of nitrogen at constant temperature, in L. Stanley et al. (eds.), *Proc. Symp. on Laser Materials Processing ICALEO 90, Boston, Massachusetts, USA, November 4–9, 1990*, Laser Institute of America, Orlando, FL, 1991, pp. 525–538.

[18] A. Karimi and M. Maamouri, Microscopic study of cavitation erosion in copper and Cu–5.7% Al single crystals, *Wear, 139* (1990) 149–169.

[19] A. Ball, On the importance of work hardening in the design of wear-resistant materials, *Wear, 91* (1983) 201–207.